Evaluating the Uncertainty of Area Estimates Derived from Fuzzy Land-Cover Classification

Frank Canters

Abstract

The use of remotely sensed data as input into geographical information systems has promoted new interest in issues related to the accuracy of multispectral classification. This paper investigates the impact of classification uncertainty on the estimation of area from satellite derived land-cover data. Applying four variants of the maximum-likelihood classifier, it is shown that the estimated area for different land-cover classes is highly influenced by the methods which are used for classifier training. To evaluate the uncertainty of area estimates, a new error modeling strategy is proposed. Assuming that attribute uncertainty in image classification is field-based rather than pixel-based, the image is segmented in fields according to similarities in the probability vectors of adjacent pixels. In simulating uncertainty, this field structure is explicitly taken into account. Using different strategies for image segmentation, it is shown that the spatial correlation of classification uncertainty has a major impact on the assessment of the uncertainty of area estimates.

Introduction

Since the launch of high-resolution remote sensors, the use of satellite images as a major source of spatial information has been the subject of extensive research in a broad range of applications. As a result of these research efforts today, the benefits of high-resolution remote sensing technology are widely recognized. In particular, the extraction of land-cover information from remotely sensed data has received considerable attention over the last ten years and has become almost common practice in many application areas. A wide range of classification approaches for the extraction of land-cover information has been developed, and many strategies and modifications have been proposed to improve classification accuracy obtained with these classifiers.

In most classification studies, map accuracy is assessed by means of a confusion matrix which compares a sample of the classified pixels with reference data obtained from aerial photographs or ground surveys. In recent years many authors have commented on the shortcomings of the confusion matrix as an estimator of classification accuracy. Much work has been published on optimal strategies for ground truth sampling, accuracy measures have been refined to deal with chance agreement, and methods have been presented to estimate statistically sound classification probabilities from the confusion matrix (van Genderen, 1978; Rosenfield *et al.*, 1982; Congalton, 1988; Foody, 1992; Stehman, 1992; Green *et al.*, 1993; Stehman, 1995). Yet the most fundamental drawback of the confusion matrix is its inability to provide information on the spatial structure of the uncertainty in a classified scene. Measures of uncertainty and class membership probabilities can only be derived for a land-cover class as a whole and are considered as representative for each pixel that is assigned to that class, thereby ignoring the complex spectral response that is present in a multispectral satellite image.

Today much attention is given to error modeling and error propagation in GIS databases. The motivation behind this research is the general acknowledgment that a successful use of GIS as a decision support tool can only be achieved if it becomes possible to attach a quality label to the output of each GIS analysis. Most commercial GIS packages do not provide tools for the modeling of error in individual data layers and for the tracking of error when data layers are manipulated and combined in a GIS-based spatial analysis. Yet the issue of spatial data uncertainty is given high priority on the GIS research agenda and is one of the most frequently covered topics in recent scientific literature on GIS. With the increasing use of remotely sensed data as input into geographical information systems, the accuracy of multispectral classification also gained more attention and new approaches were taken to describe and model the uncertainty that characterizes the classification process.

One of the most frequently used techniques to study the effect of uncertainty in source data on the quality of GIS-derived products is Monte Carlo simulation modeling. Starting from a number of assumptions regarding the magnitude and spatial distribution of error in the source layers involved, each of these layers is randomly sensitized with error. Applying a sequence of GIS functions to the perturbed data layers yields an output that differs from the result obtained with the original source data. Repeating this process M times yields a set of M different output layers which allows characterization of the uncertainty that is present in the result of the analysis. If the output of the analysis is numerical, e.g., area estimates of different map categories, summary statistics can be derived. While the mean value obtained for the area of each category can be used as an estimate of the area that is actually occupied by that category, the variance of these estimates gives an indication of the uncertainty that is involved.

Monte Carlo simulation is computationally intensive yet it has the advantage of being universally applicable to any type of GIS analysis, regardless of its nature or complexity. This is the main reason why it has been used so frequently in recent error propagation studies emanating from a broad range of applications and dealing with, for example, the derivation of gradient and aspect (Heuvelink *et al.*, 1990; Canters, 1994), viewsheds (Fisher, 1992), and floodplains (Lee *et al.*, 1992) from digital terrain models; the valuation of land from land-use and soil information (Fisher, 1991); the model-

Centre for Cartography and GIS, Department of Geography, Vrije Universiteit Brussel, Pleinlaan 2, B 1050 Brussel, Belgium.

Photogrammetric Engineering & Remote Sensing, Vol. 63, No. 4, April 1997, pp. 403–414.

0099-1112/97/6304-403$3.00/0

ing of forest growth (Mowrer, 1994); and the selection of suitable sites for nuclear waste disposal (Brunsdon *et al.*, 1990). Goodchild and Wang (1988) suggested the use of class membership probabilities for the stochastic modeling of the uncertainty inherent to statistical image classification. Traditionally, the output of classification is an image in which each pixel is assigned to the most likely class, i.e., the one with the highest probability. Class membership probabilities on which the assignment is based are usually disregarded. It is obvious that in doing so a lot of valuable information on classification uncertainty is lost.

This study presents a new method for the stochastic modeling of classification uncertainty. Starting from a common application, the derivation of area estimates from land-cover classification, it will be shown how our conception of classification uncertainty affects area estimation as well as the assessment of the uncertainty of area estimates. Assumptions about the nature of classification uncertainty are reflected in the classification procedures we use as well as in the definition of the stochastic error model on which the assessment of uncertainty is based. In this paper we will first discuss different approaches to statistical image classification and evaluate their impact on the estimation of area. Next we will propose a new strategy for uncertainty assessment which makes optimal use of class membership probabilities. The proposed method will be applied to a small test area situated along the Belgian-Dutch border, northwest of the city of Ghent.

Traditional Approaches to Image Classification

Most classification methods assume that an image scene can be decomposed into a small number of spectrally separated classes, each of which can be allocated to a well-defined type of land cover. This corresponds to a model of the Earth's surface that consists of a collection of homogeneous patches of land with precise boundaries and a unique combination of properties that can be related to a particular land-cover type. Changes are supposed to occur only along patch boundaries. In reality, however, changes in land cover are less abrupt and the definition of different land-cover classes is more ambiguous. For example, vegetation classes tend to inter-grade gradually, making it very difficult to assign part of a transition zone to one vegetation class (Foody *et al.*, 1992). This problem of class definition is encountered in visual as well as in digital image interpretation. It points at the inability of Boolean classification methods to properly deal with the mapping of continua.

In agricultural areas, land-cover classes are in general more easy to define. Sometimes, however, they are a mixture of different cover types. For example, orchards have a heterogeneous structure due to the regular alternation of tree canopy and grassland filling the space in between the trees. As such they are usually easy to identify by visual interpretation of aerial photographs. In digital image processing the typical alternation of cover type might be detected by introducing texture as an extra feature in the classification procedure, yet the success of this approach highly depends on the resolution of the imagery. Strahler *et al.* (1986) make a distinction between high-resolution and low-resolution scene models, depending on whether the resolution cells of the image are smaller or larger than the elements in the scene. In the high-resolution case, elements that are part of a heterogeneous class may be individually resolved. In the low-resolution case, different cover types that are part of the same class will contribute to the spectral reflectance values of individual pixels, thus blurring the distinctive texture of the class and impeding a clear spectral definition. This problem of mixed pixels, of course, also occurs along the boundaries between different land-cover classes. In zones of highly heterogeneous land use such as suburban areas, the occurence of mixed pixels often makes it difficult to obtain spectrally dissimilar class signatures and may ultimately lead to a low proportion of correctly classified pixels.

Problems with traditional classification methods are essentially due to the inability of these methods to deal with attribute uncertainty for individual pixels. This is reflected in the methods that are used for the determination of class signature as well as in the classification procedures themselves. In supervised classification the description of each class is based on the statistics obtained from a set of training pixels which are considered to be representative for that class. These pixels are regarded as "pure" in two ways. First of all, it is assumed that only one type of land cover occurs within the boundaries of these pixels. Secondly, no doubt is entertained as to the class to which these pixels actually belong. Now, even if we suppose that individual land-cover classes can be defined in an unambiguous way, which may be the case for some classes (e.g., water) but which is certainly questionable for others (e.g., residential area), the problem still remains as to how representative pixels, so far as they exist at all, should be selected. Especially in the low-resolution case, the occurrence of perfectly homogeneous pixels will be rare and a clear spectral definition of land-cover classes from selected training pixels will be hampered by small inclusions of other cover types and spatially homogeneous mixing at the subpixel level.

Once spectral signatures are defined, supervised classification assigns each pixel in the image to exactly one spectral class using a discriminant function which may be based on the measurement of spectral distance (parametric methods) or on the frequency histograms of the classes considered (nonparametric methods). Although some of these methods (e.g., the maximum-likelihood classifier) produce class membership probabilities for each pixel, they are basically grounded on the concepts of classical set theory. While it may be tempting to consider the class membership probabilities of the traditional maximum-likelihood classifier as indicative of class mixture at the subpixel level, it remains questionable if reliable conclusions on fuzzy membership can be drawn from the output of a supervised classification procedure which generates spectral signatures from training pixels that are entirely assigned to *a priori* defined cover types through a hard classification procedure. Traditional unsupervised classification methods show the same inadequacy to deal with attribute uncertainty. By means of a clustering algorithm, spectral space is iteratively partitioned into regions, each of which corresponds to one spectral class. Pixels inside a region are considered as entirely belonging to that class. After classification no information on the probability of class membership is available.

Fuzzy Approaches to Image Classification

Fuzzy logic is increasingly used for the handling of uncertainty in geographical databases (Burrough and Frank, 1996). Building on concepts of fuzzy set theory, new methods for accuracy assessment have been presented (Gopal and Woodcock, 1994) and new classification approaches have been developed to properly deal with uncertainty in class allocation. Starting from the assumption that each training pixel can contribute to the spectral signature of each predefined class, Wang (1990a; 1990b) modified the traditional maximum-likelihood classifier by calculating a fuzzy mean and a fuzzy covariance matrix for each class. The fuzzy mean is given by

$$\boldsymbol{\mu}_i^F = \frac{\sum_{j=1}^{n} f_i(\mathbf{x}_j)\mathbf{x}_j}{\sum_{j=1}^{n} f_i(\mathbf{x}_j)} \qquad (1)$$

where n is the total number of training pixels, $f_i(\mathbf{x})$ is the membership function of class i, and $\mathbf{x}_j$ is the jth pixel measurement vector, containing the brightness values of the pixel in each spectral band. The fuzzy covariance matrix is given by

$$\mathbf{\Sigma}_i^F = \frac{\sum_{j=1}^{n} f_i(\mathbf{x}_j)(\mathbf{x}_j - \boldsymbol{\mu}_i^F)(\mathbf{x}_j - \boldsymbol{\mu}_i^F)^T}{\sum_{j=1}^{n} f_i(\mathbf{x}_j)} \quad (2)$$

As can be seen, the contribution of each training pixel to the fuzzy mean and fuzzy covariance of a class i is determined by its membership value. For each training pixel, all membership values should be positive and add up to 1. A membership value close to 1 indicates that the pixel almost certainly belongs to that class; a value close to 0 indicates that the pixel is very unlikely to belong to that particular class. The membership values for each training pixel can be taken from a previously determined classification which is in a fuzzy representation (Wang, 1990a) or can be derived from the class membership probabilities of a traditional maximum-likelihood classification of the same image (see below). Once fuzzy class signatures have been determined, the standard maximum-likelihood procedure is applied, except that the mean and covariance matrices in the definition of the probability density function for each class are replaced by their fuzzy counterparts. The probability density function for class i thus becomes

$$p(\mathbf{x} \mid i) = (2\pi)^{-N/2} \mid \mathbf{\Sigma}_i^F \mid^{-1/2} \exp(-0.5(\mathbf{x} - \boldsymbol{\mu}_i^F)^T (\mathbf{\Sigma}_i^F)^{-1} (\mathbf{x} - \boldsymbol{\mu}_i^F)) \quad (3)$$

where N is the number of spectral bands used in the classification.

In contrast to traditional supervised approaches, where class signatures are obtained by hard classification of a set of training pixels, the use of fuzzy sets throughout the entire process of image classification ensures that the class membership values for each pixel in a classified scene can be interpreted as the probabilities of a fuzzy event. As Wang (1990a) demonstrated, class membership values produced by the fuzzy classifier allow correct assessment of the proportions of component classes in a pixel. Other fuzzy classification methods have also been proposed. Bezdek *et al.* (1984) developed a fuzzy c-means (FCM) clustering algorithm that has been used with success in the unsupervised classification of remote sensing data (Cannon *et al.*, 1986). In a study on land-cover mapping in suburban areas, Fisher and Pathirana (1990) demonstrated that also for the fuzzy c-means classifier the proportion of the area of a pixel that is occupied by a particular type of land cover is highly correlated with the fuzzy membership value of that class. However, as the experiments which are described in this paper are all based on supervised classification, alternative approaches, which may be equally useful or even more appropriate in some cases, will not be given further consideration here.

Indicators of Classification Uncertainty

Before evaluating the accuracy of a classified land-cover scene or the quality of the outcome of a GIS analysis in which satellite derived land-cover data are used, it should be clear what type of accuracy one is attempting to measure. Possible disturbances that may occur during the registration of the satellite image as well as the processes involved in its sequential treatment will all contribute to the accuracy of the classification. As such, the assessment of classification accuracy is a complex matter. This complexity is reflected in the many strategies and accuracy measures that have been proposed in the past. The use of different terminologies to address the issue of classification accuracy, including terms like precision, uncertainty, and reliability, only adds to the confusion. While all these concepts have a clear meaning, they are often mixed up (Janssen and van der Wel, 1994).

The most obvious way of assessing classification accuracy is by comparing the class assigned to a pixel in the classification with the corresponding class observed in the field. The comparison of the classified land-cover to the actual land-cover is usually recorded in a confusion matrix. For each land-cover class the confusion matrix reports the number of pixels that are classified into class i but actually belong to class j (commission errors) as well as the number of pixels that belong to class i but are wrongly assigned to class j (ommission errors). From the confusion matrix global or class-dependent measures of accuracy are derived by dividing the number of correctly classified pixels by the total number of pixels in the sample. Methods have been presented to estimate statistically sound class membership probabilities from the confusion matrix, taking into account the sampling strategy that is applied (Green *et al.*, 1993). Estimated probabilities derived in this way are, however, identical for all pixels that have been assigned to the same class. Hence, no information about the spatial distribution of classification reliability within the classes is available.

Alternatively, as was already mentioned, one might consider the probabilities that are generated by statistical classification as indicators of the reliability of pixel assignment. In maximum-likelihood classification it is assumed that the spectral signature of a class i can be approximated by the multivariate normal distribution with the probability density function for that class given by Equation 3. According to Bayes theorem, the probability that the assignment of a pixel at $\mathbf{x}$ to class i is correct is then given by

$$p(i \mid \mathbf{x}) = \frac{p(\mathbf{x} \mid i)p(i)}{p(\mathbf{x})} \quad (4)$$

where $p(i)$ is the probability that class i occurs in the image and $p(\mathbf{x})$ is the probability of finding a pixel from any class at location $\mathbf{x}$ (Richards, 1986, p. 175). In mathematical terms $p(\mathbf{x})$ can be written as follows:

$$p(\mathbf{x}) = \sum_{i=1}^{m} p(\mathbf{x} \mid i)p(i) \quad (5)$$

where m is the number of classes. The $p(i)$ are called prior probabilities. They represent the chance that a pixel in the image belongs to a given class, irrespective of its spectral characteristics. In the literature several methods have been proposed for the assessment of prior probabilities (Strahler, 1980). If no external information on the study area is available prior to the classification, the value of $p(i)$ is usually kept constant for all classes. In that case, Equation 4 simplifies to

$$p(i \mid \mathbf{x}) = \frac{p(\mathbf{x} \mid i)}{\sum_{j=1}^{m} p(\mathbf{x} \mid j)} \quad (6)$$

The advantage of working with class membership probabilities produced by statistical classification is that these probabilities provide information on classification reliability at the level of each individual pixel. Immediately it should be pointed out, however, that probabilities derived in this way cannot be considered as pure indicators of classification accuracy as they only reflect the uncertainty that is inherent to the statistical classification procedure itself, therefore not taking into account all problems related to the definition of the class signatures on which the classification is based. In contrast, the indices that are derived from the confusion ma-

trix can be considered as direct measures of the accuracy of the classification because they reflect the overall impact of all possible errors that may have occurred in the sequential processing of the image. Hence, it is probably more correct to speak of classification uncertainty instead of classification accuracy when using class membership probabilities from the maximum-likelihood classifier to evaluate the result of a classification. This inconvenience does not detract from the usefulness of these indicators. The accuracy of classification can only be verified in the field and, as such, is necessarily restricted to global assessment based on statistical sampling. For the purpose of error modeling, this may prove more restrictive than the indirect measurement of classification accuracy by way of the uncertainty that follows from statistical classification.

Some authors have used maximum-likelihood membership probabilities to evaluate the reliability of a classification. Foody *et al.* (1992), for example, demonstrated how class membership probabilities may be used to improve the quality of a classification by identifying areas that are less satisfactorily classified. Maselli *et al.* (1994) defined a new measure which they called "relative probability entropy" to express the heterogeneity of class membership probabilities and used it as an indicator of classification uncertainty. As was already mentioned, the Fuzzy c-Means classification algorithm also produces class membership values. Fisher and Pathirana (1993) used FCM membership values to improve the results of change detection from multitemporal satellite imagery. Class membership values also offer interesting opportunities for the visualization of uncertainty. In a recent paper, Fisher (1994) presented a new method for the dynamic display of classification reliability which is based on the random assignment of classified pixels to other cover types, depending on their class membership values.

The value of class membership probabilities derived from the maximum-likelihood classifier as indirect indicators of classification accuracy will increase if additional measures are taken for a better definition of class signatures. In this study a robust variant of the maximum-likelihood classifier has been applied. Robust estimators give less weight to atypical pixels when determining the mean and covariance matrix from the sample data. This increases the spectral separability of the class signatures. The most frequently used robust estimator is the so-called M-estimator which takes the form of a weighted average. Using this estimator, the expressions for the mean and the covariance matrix for a class i, respectively, become

$$\boldsymbol{\mu}_i^M = \frac{\sum_{j=1}^{n} w_{ij}\,\mathbf{x}_j}{\sum_{j=1}^{n} w_{ij}} \tag{7}$$

and

$$\boldsymbol{\Sigma}_i^M = \frac{\sum_{j=1}^{n} w_{ij}^2\,(\mathbf{x}_j - \boldsymbol{\mu}_i^M)(\mathbf{x}_j - \boldsymbol{\mu}_i^M)^T}{\sum_{j=1}^{n} w_{ij}^2 - 1} \tag{8}$$

with w_{ij} the weight that is associated with the jth pixel in the sample.

Weights have to be calculated on the basis of the atypical character of the observation with respect to the mean and covariance matrix that need to be estimated. Due to this interdependence, weights have to be determined by iteration. The class typicality of a pixel is negatively related to the distance between the pixel and the class centroid and is usually measured by means of the Mahalanobis distance

$$d_{ij} = \{(\mathbf{x}_j - \boldsymbol{\mu}_i)^T\,\boldsymbol{\Sigma}_i^{-1}\,(\mathbf{x}_j - \boldsymbol{\mu}_i)\}^{1/2}\,. \tag{9}$$

In this study, weights were calculated using the distance decay function suggested by Campbell (1980): i.e.,

$$w_{ij} = \begin{cases} 1 & d_{ij} \le d_0 \\ \dfrac{d_0}{d_{ij}} \exp\left\{-\dfrac{1}{2b_2^2}\,(d_{ij} - d_0)^2\right\} & d_{ij} > d_0 \end{cases} \tag{10}$$

with

$$d_0 = \sqrt{N} + \frac{b_1}{\sqrt{2}}\,. \tag{11}$$

N is the number of spectral bands used in the classification, and b_1 and b_2 are two constants with a value of 2.00 and 1.25, respectively, as recommanded by Campbell. As can be seen, observations which are close to the class centroid receive full weight. These are the observations which are considered to be representative of the class. As the Mahalanobis distance increases, weights will decline accordingly.

One may have noticed that the robust estimators (Equations 7 and 8) somewhat resemble the definition of the fuzzy mean and fuzzy covariance matrix (Equations 1 and 2) (both are weighted means). However, there is a clear difference between both. While the robust mean and robust covariance matrix are calculated from class-specific training samples, the fuzzy mean and fuzzy covariance matrix for each class are derived from the complete set of training data. Although robust estimation deals with atypical training pixels, it does not recognize the fact that pixels may contribute to the spectral signature of more than one class.

Estimating the Area of Different Land-Cover Classes

Estimation of the area of different cover types in a classified scene is one of the most well-known operational applications of remote sensing. Area estimation often has economic implications, for example, when assessing total area and potential yield for different crops in connection with agricultural policy monitoring. It is, therefore, important that attention be paid to the quality of area estimation. First of all, one should strive to obtain area estimates for the different classes in the image which are as close as possible to the real proportion taken by each class. On the other hand, it is important to quantify the reliability of the estimates, which may differ from one class to another, in order to be able to evaluate the usefulness of the estimates and to decide if additional measures should be taken to obtain better results. This paper focuses on area uncertainty assessment. However, because estimation of area uncertainty cannot be detached from area estimation itself, we will first look at a number of techniques that can be applied for the derivation of area estimates from classified satellite data.

The easiest way to derive area estimates from a classified image is by simply counting the number of pixels that have been allocated to each of the classes in the hard classification result. This is common practice, yet it is clear that area estimates obtained in this way will be biased as a result of classification error. Although measures to improve classification accuracy will also improve area estimation, some bias will always remain. Statistical methods based on classical and inverse calibration have been applied to correct area estimates for misclassification bias using error information from the confusion matrix (Bauer *et al.*, 1978; Card, 1982; Prisley and Smith, 1987). Recent studies have indicated that the inverse estimator is consistently superior to the classical estimator with respect to bias and precision (Czaplewski and Catts, 1992; Walsh and Burk, 1993). Inverse calibration is rel-

atively easy to apply. Let us consider a sample of n pixels which are classified into one of m categories using remote sensing, and which are also independently labeled by field survey. From this sample, a confusion matrix **C** can be constructed, with each element c_{ij} indicating the number of pixels that are classified into class i but actually belong to class j. Let **R** represent an (m by m) diagonal matrix with its ith element equal to the number of pixels in the sample classified into class i, and **r** be an (m by 1) vector of the total number of pixels in the image allocated to each class. Then the inverse estimator **t** of the true number of pixels in each class is given by

$$\mathbf{t} = (\mathbf{C}' \mathbf{R}^{-1}) \mathbf{r} \tag{12}$$

where $(\mathbf{C}'\mathbf{R}^{-1})$ is a matrix of conditional probabilities with its ijth element indicating the probability $p(t_i \mid c_j)$ that the true class of a pixel is i given it is classified into j. Column vectors in this matrix each sum to 1. Czaplewski and Catts (1992) recommend a minimum of 500 to 1000 randomly chosen samples for inverse calibration, assuming, of course, that the confusion matrix is truly representative of the classification. If misclassification error is different for various subregions, the area should be properly stratified and calibration should be applied to each of the strata.

Both classical and inverse calibration require reference data that are independent of the data used to train the classifier. For the case study presented in this paper, not enough samples were available for calibration. For that reason, the area of each class was calculated directly from the maximum-likelihood classification of the image. Because the maximum-likelihood classifier assigns each pixel to the most likely class, it is clear that the proportion of different land-cover classes in a classified image will deviate from the actual area that is covered by each class. Categories that occur frequently as the most likely class, yet with low class membership probabilities, will be overestimated. Categories that are often present as the second most likely class, with probabilities that are not negligible, will be systematically underestimated. To reduce this bias, the area of a class i was estimated as follows:

$$A_i = \sum_{j=1}^{n} p(i \mid \mathbf{x}_j) a \tag{13}$$

where $p(i \mid \mathbf{x}_j)$ is the probability of class i for pixel $\mathbf{x}_j$, n is the total number of pixels in the image, and a is the area that is covered by each pixel.

Of course, it is not possible to guarantee that area estimates derived from Equation 13 are truly unbiased. First of all, Equation 13 assumes that class membership probabilities for mixed pixels are directly related to the proportion of sub-pixel component classes. While Wang (1990a) observed a strong correspondence between class membership probabilities derived from fuzzy maximum-likelihood classification and class proportions, the strength of the relationship will much depend on the characteristics of the training data. If class signatures are not representative of the cover type because of poor quality reference data, or if class distributions strongly deviate from multinormality, it is questionable if the correlation between membership probabilities and class proportions will still be marked. On the other hand, the mixed pixel interpretation of Equation 13 is somewhat simplistic because it does not consider the effects of spectral confusion between classes. If unbiased area estimates are to be derived from linear models of the type of Equation 13, again some calibration technique should be applied. Some interesting work has already been done in this area. Foody (1994) used regression analysis to estimate sub-pixel forest cover from spatially degraded Landsat MSS data using forest cover estimates derived from the original Landsat data as a reference, and obtained a strong correlation between predicted and actual forest cover. Pech *et al.* (1986) applied different multivariate calibration methods (Brown, 1982) for estimating sub-pixel vegetation cover with a linear composite reflectance model. Similar methods might be followed to model the relationship between class proportions and class membership probabilities when more than two image classes are involved.

Which techniques one can apply for area estimation will depend on the type of information about error or uncertainty that is available. Area calibration at sub-pixel level, as described above, may be an interesting alternative to global calibration methods, especially if area estimates for smaller sub-regions are required, yet it can only be applied if spatially more detailed reference data (e.g., higher resolution satellite data) are available for a representative part of the area. If this is not so, inverse or classical calibration can be applied using information contained in the error matrix. If ground truth is insufficient to derive a reliable error matrix (see above), no calibration will be possible. In that case, however, one can still use Equation 13 for the derivation of area estimates. Indeed, referring to the observed correspondence between membership values and class proportions in previous studies, the use of membership probabilities for area estimation, applying Equation 13, is likely to produce more reliable estimates of area than simply counting the number of pixels for each class. Due to a lack of reference data, this is also the method that has been applied in this study. In the following we will look at the impact of different variants of the maximum-likelihood classifier on the estimation of area, using pixel counting as well as probability weighting. Next, a new method for the quantification of the reliability of area estimates will be proposed. Although in this paper the method will only be demonstrated in connection with uncalibrated area estimation, it should be mentioned that the technique can also be used to assess the uncertainty of area estimates that are obtained by inverse calibration (see Equation 12).

Application

Area estimation was applied to a subset of a geometrically corrected Landsat image, located along the Belgian-Dutch border, northwest of the city of Ghent, and covering an area of 13 by 13 km (Lambert coordinates: LL 210495N, 96010E; UR 223480N, 109000E). The study area is partly situated in the Scheldepolders (upper part of the image), partly in the Meetjesland (lower part), and is characterized by a highly fragmented pattern of land use. Using a maximum-likelihood approach, the image was classified into 11 categories which were regrouped into five major types of land cover (forest, grassland, agriculture, built-up area, and water) (Figure 1a). Spectral signatures were obtained by stratified random sampling from two training areas (100 by 100 pixels each), one located in the Scheldepolders, the other in the Meetjesland. Only for water was the signature derived from a non-supervised classification (ISODATA) as the number of pixels in the training areas belonging to this class was too small to obtain a representative class signature. For the other classes, spectral signatures were determined using four different approaches: normal, robust, fuzzy, and fuzzy robust estimation. The principles of fuzzy and robust classification have been described earlier in this paper. As no reference classification was available for the study area, class membership probabilities produced by the conventional maximum-likelihood classifier were used to indicate to what extent each training pixel contributes to the fuzzy mean and fuzzy covariance matrix of the different classes. Fuzzy robust estimation of class signatures, as proposed by Vandeneede *et al.* (1995), combines the advantages of fuzzy and robust estimation pro-

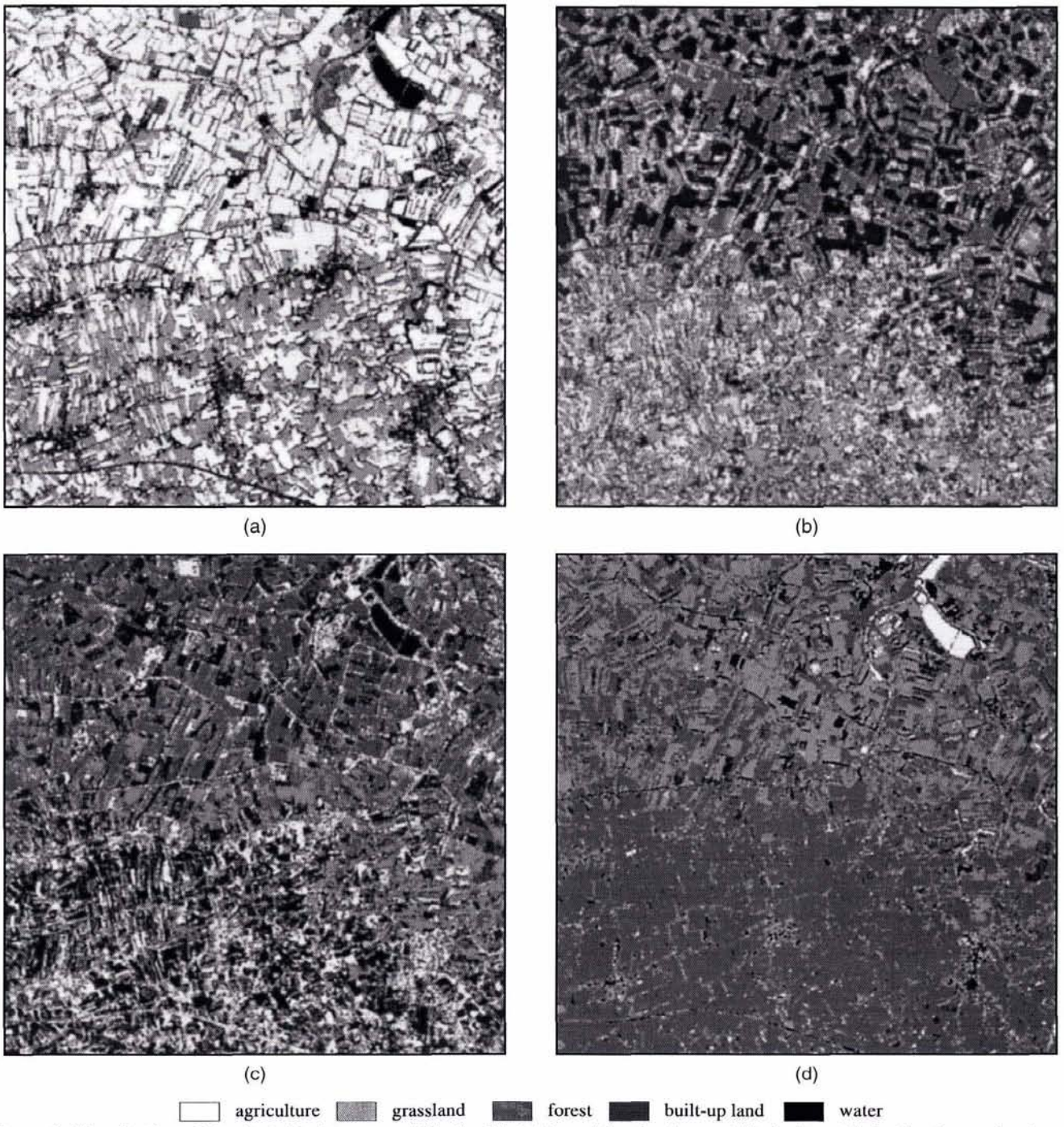

Figure 1. Visualization of the first (a), the second (b), the third (c), and the fourth most likely class (d) for the fuzzy robust maximum-likelihood classification of the study area.

cedures. The only difference with fuzzy classification is that membership values for the training pixels are based on robust instead of conventional estimation of sample mean and covariance matrix. After classification, pixel probabilities for the 11 initial categories calculated from Equation 6 were combined to obtain membership values for the five major types of land cover.

For each classification strategy (normal, robust, fuzzy, and fuzzy robust), total area was estimated for the five major types of land cover. Table 1 reports the area for each land-cover class, calculated by simply counting the total number of pixels assigned to each class. It is immediately clear that the way in which class signatures are determined has a non-negligible impact on the estimation of area. With robust estimation of spectral signatures, the area of built-up land seems to increase compared to conventional classification results. One of the reasons for this turned out to be the limited presence of homogeneous pixels of built-up area in the training sample, which leads to a less clear signature for this class strongly overlapping with the signatures for the other classes (especially agricultural land). On the other hand, the road infrastructure that appears within the area defined by the train-

TABLE 1. AREA (HA) FOR EACH LAND-COVER CLASS BY PIXEL COUNT

	forest	grassland	agriculture	built-up land	water
normal	1050.28	3999.64	9147.36	2561.48	141.24
robust	1022.40	3952.76	8801.28	2982.32	141.24
fuzzy	1109.48	3932.76	8700.52	3016.00	141.24
fuzzy robust	1032.76	3897.16	8631.92	3196.92	141.24

TABLE 2. AREA (HA) FOR EACH LAND-COVER CLASS BY PROBABILITY WEIGHTING

	forest	grassland	agriculture	built-up land	water
normal	1051.48	3882.96	9351.64	2471.96	141.96
robust	1025.72	3578.76	9306.88	2846.68	141.96
fuzzy	1164.48	3806.08	8859.76	2927.72	141.96
fuzzy robust	1083.84	3781.76	8790.36	3102.08	141.96

ing plots was not registered as such. Mixed pixels which partly belong to the road network therefore contributed to the spectral signature of all classes. Robust estimation of signatures narrows the spectral definition of the different cover types. This explains why a lot of mixed pixels which were originally assigned to other cover classes are now assigned to built-up area. Fuzzy estimation of class signatures has a similar effect, again indicating that there is a strong spectral confusion between built-up area and the other cover classes. Fuzzy robust estimation combines both strategies. This is also reflected in the results of area estimation. The estimated area for water always remains the same no matter what strategy is applied, which proves that water has a very distinctive signature that is not easily confused with other classes.

The confusion between different cover types becomes apparent when, next to the most likely class, the second most likely class (Figure 1b) as well as the probability of occurrence of the most likely class are displayed (Figure 2). The latter gives an idea of the trust that can be put in the assignment of a pixel to the most likely class. As could be expected, uncertainty in the classification mainly occurs along the edges of the parcels. The detailed structure of the parcels in the Meetjesland brings about a relatively high degree of uncertainty in the southern part of the image. In particular, built-up area is characterized by high classification uncertainty. Where pixels are assigned to built-up area, it is mainly agricultural land (and to a lesser extent forest area) which occurs as the second most likely class. This confirms the sensitivity of area estimation for agricultural land and built-up area to the way in which class signatures are determined.

Table 2 reports the area which is obtained for each land-cover class if membership probabilities are taken into account in the estimation (Equation 12). Compared with the results shown in Table 1, estimated values are higher for forest and agricultural land, lower for grassland and built-up area, and this for all variants of the maximum-likelihood classifier. Again, this is easily explained when looking at the spatial distribution of uncertainty. Forest and agricultural land often occur as the second most likely class in pixels with a relatively low first likelihood probability. Grassland and especially built-up area are also present in the second likelihood image, yet mostly in pixels with a high first likelihood probability. For water the use of class membership values has no major impact on area estimation. As the probability map shows, hardly any uncertainty is involved in the assignment of pixels to this class. Of course, one cannot attach significance to the changes in area estimates in Tables 1 and 2 without having any notion of the reliability of these estimates. The results of the uncertainty assessment which will be discussed below, however, will make it clear that the changes which have been observed are meaningful. Hence, we may conclude that the use of fuzzy and robust techniques for classifier training may have a significant impact on the estimation of area. Unfortunately, in this case study it could not be verified which of the four methods produced the best results because true areal proportions were unknown.

Modeling the Uncertainty of Area Estimates

Although Equation 13 produces estimates of the area of each land-cover class taking into account the uncertainty of pixel assignment, it does not give an indication of the reliability of these estimates. To evaluate the impact of classification uncertainty on area estimation, Monte Carlo simulation has been applied. Simulation modeling in connection with image classification requires the definition of a mechanism that generates multiple versions of the classified image in such a way that the marginal distribution in each pixel corresponds with the class membership probabilities produced by the classifier. For example, if a pixel has a probability of 0.8 for grassland, one has to make sure it is assigned to that class in approximately 80 percent of all simulated coverages. If it is assumed that all pixels are independently assigned to a land-cover class, it is relatively easy to define a stochastic process which satifies this requirement. As class membership probabilities always add to one, each class can be matched to a sub-interval in the range 0 to 1 with its length proportional to the probability of that class. Generating a uniformly distributed random number in the range 0 to 1 and assigning the pixel to the class that corresponds with the interval including this randomly drawn number ensures that class membership probabilities for each pixel are respected across a large number of realizations (Figure 3) (Goodchild and Wang, 1989).

Figure 4 shows an enlargement of a small section of the fuzzy robust classification of the test area (a) together with

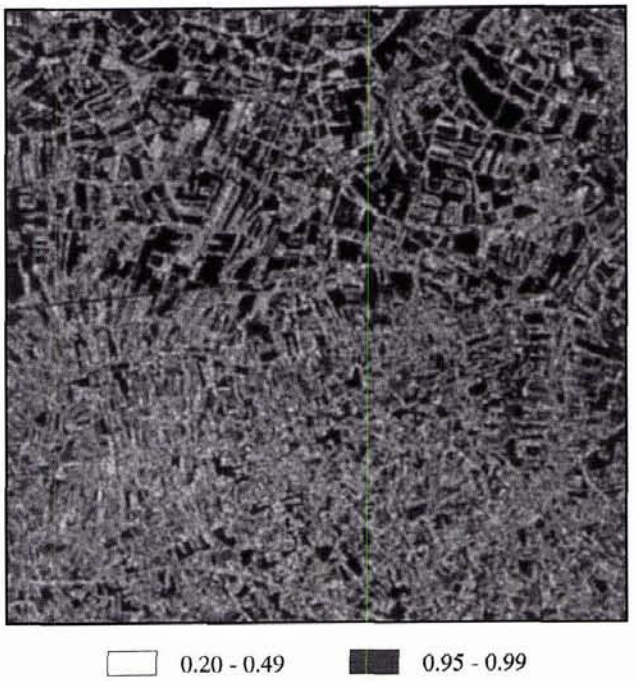

Figure 2. Probability of the most likely class.

the corresponding probability image (b). Figure 5a shows an example of a simulated classification which was generated from the class membership probabilities of the fuzzy robust classifier using the approach just described. Although the simulated coverage resembles the original outcome of the classification, the image is highly fragmented in areas with low first likelihood probabilities. This is a result of the independence of the outcome in neighbouring pixels. Still, if one wants to assess the impact of image classification uncertainty on the output of some GIS analysis using Monte Carlo simulation, it is of utmost importance that the simulated coverages can be considered as good representations of the real, yet not exactly known, variation in land cover, i.e., as being part of the same statistical population. The simulation process should therefore not only respect class membership probabilities for each pixel, but should also take into account the structural characteristics of the land-cover scene.

In agricultural areas, as in the case study which is presented here, the Earth's surface can be considered as consisting of a collection of adjacent "fields" inside of which no major variation in cover type occurs. Uncertainty in land-cover assignment is therefore bound to a field as a whole rather than to each pixel which is part of it. In terms of image classification, this means that, if one assumes that a pixel belongs to a specific class, one has very good reasons to assume that adjacent pixels with similar spectral characteristics probably belong to the same class. To ensure that structural features of land cover are preserved in the modeling, a new strategy for simulation is proposed. Assuming that attribute uncertainty in image classification is field-based rather than pixel-based, the image is segmented in fields according to similarities in the probability vectors of adjacent pixels. In the simulation of land cover, this field structure is explicitly

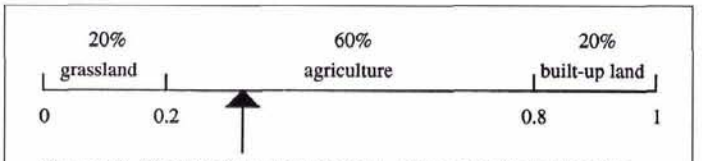

Figure 3. Mechanism for random class assignment: the sub-interval allocated to each class is proportional to the probability of that class. The pixel will be assigned to grassland if the random value is between 0.0 and 0.2, to agricultural land if it is between 0.2 and 0.8, and to built-up land if it is between 0.8 and 1.0.

taken into account. Instead of drawing a random number for each individual pixel, only one number is drawn for all pixels belonging to the same field. Based on this single drawing, each pixel is assigned to one cover type depending on its own class membership probabilities, as explained above. This mechanism still guarantees that the proportion of realizations in which a pixel is assigned to a specific class tends to its membership probability for that class. In addition to this, pixels that belong to the same field will have a high probability of being assigned to the same class. As such, the spatial structure of simulated land cover will be more realistic, at least if fields are defined in a proper way.

If we consider fields as groups of adjacent pixels with similar spectral characteristics, there is still some room left for interpretation. For instance, the grouping of adjacent pixels could be based exclusively upon the identity of the most likely class. In that case, the maximum-likelihood classifier immediately produces the field structure. However, when

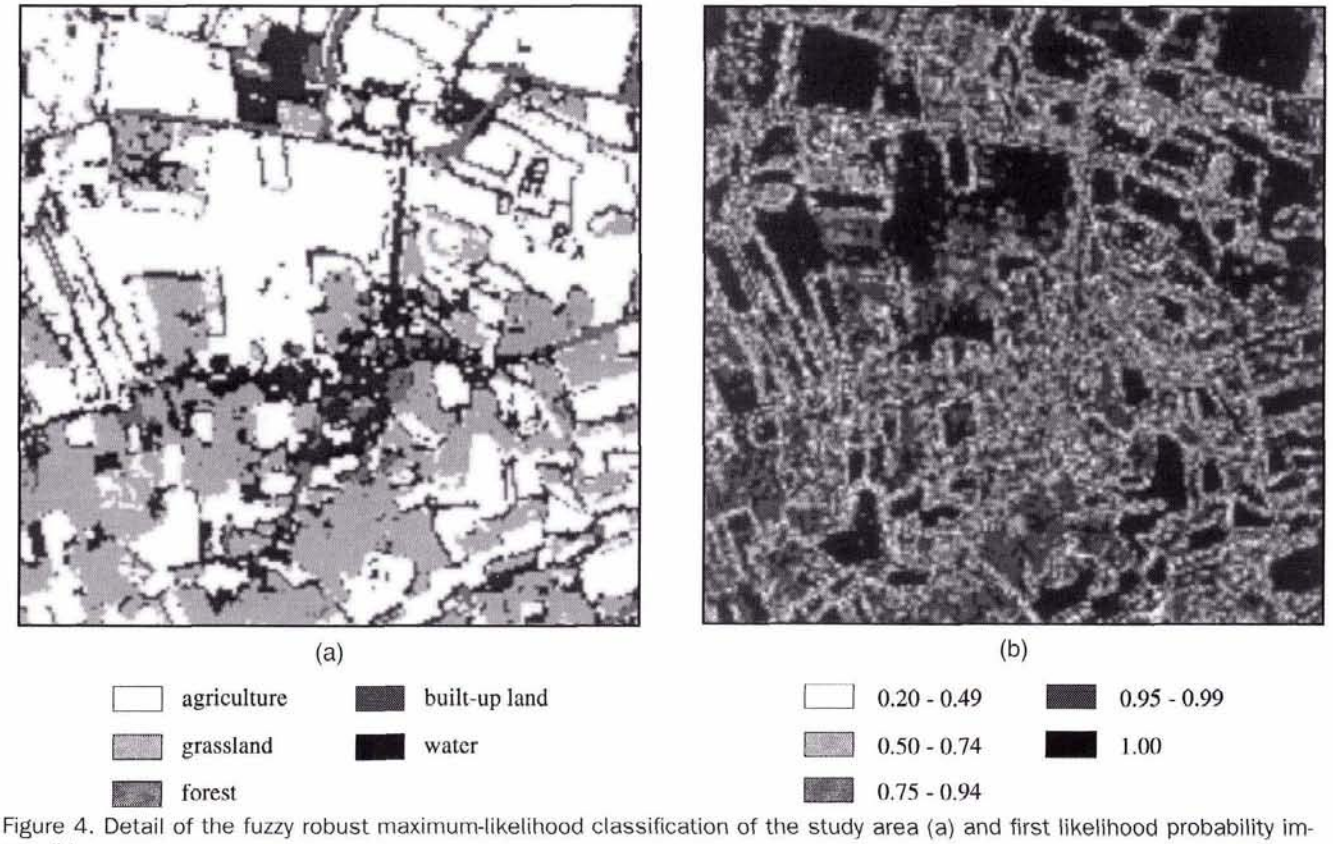

Figure 4. Detail of the fuzzy robust maximum-likelihood classification of the study area (a) and first likelihood probability image (b).

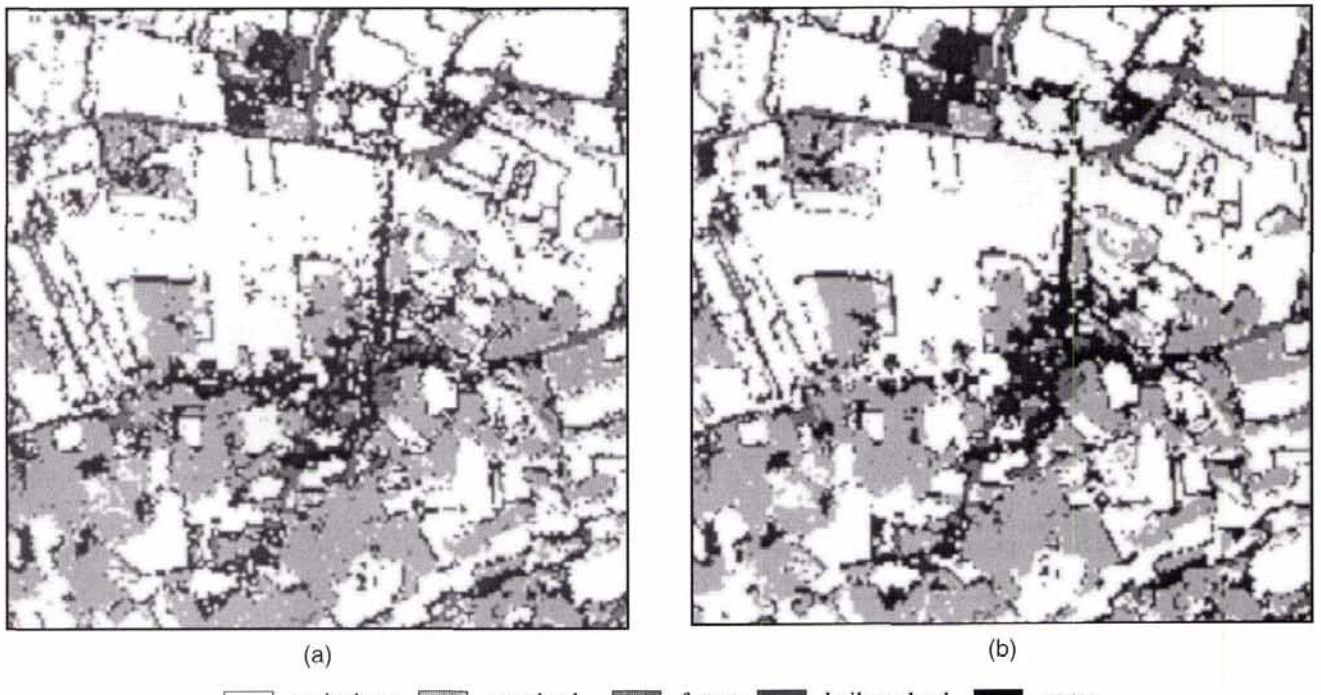

Figure 5. Two examples of simulated land-cover classifications: "pixel" approach (a) and "field" approach (b).

segmenting the image in this way, little use is made of the information on classification uncertainty which is stored in the class membership probability vectors. A relatively simple strategy which makes better use of uncertainty information consists of grouping pixels if not only the first, but also the second, third, and so on likelihood classes are the same. How many classes should be involved depends on the significance of the first, second, third, and so on most likely class. If for the majority of the pixels the sum of class membership probabilities almost equals one for the first and second most likely class, additional classes will no longer contribute to a clear identification of the field structure. Using more classes in that case would only lead to a further fragmentation of the image, thus blurring the spatial pattern of membership values. Figure 5b shows an example of a simulated classification, using a field definition that is based on the two most likely classes. As can be seen, the image is much less fragmented than the one obtained by independently assigning each pixel to a class (Figure 5a).

The grouping of pixels does not necessarily imply that all pixels which belong to the same field will also be part of the same land-cover class in each simulated classification. Although during simulation only one random number is drawn for each field, the assignment of a pixel to a class will still depend on its class membership probabilities. If these probabilities are almost alike for all pixels in the field, the chance of having all pixels assigned to the same class will, of course, be high. Yet if the differences in probability values increase, there will also be a higher chance for pixels to be assigned to other classes. As such, the result of the simulation will reflect the degree of heterogeneity within the fields. Figure 6 demonstrates class assignment within one field if there are only two classes. In the example it is assumed that class 1 is the most likely class (membership probabilities are given in Figure 6a). Figures 6b, 6c, and 6d show the outcome of the simulation process for three different random drawings r (0.55, 0.65, 0.75). Pixels are allocated to class 1 if the value of r is smaller than the first likelihood probability, to class 2 if the value of r is larger. Because membership probabilities for adjacent pixels are very alike, pixels will be assigned to both classes in only 10 percent of the realizations ($0.60 < r < 0.70$). In 60 percent of the cases all pixels will be assigned to the most likely class ($r < 0.60$), and in the re-

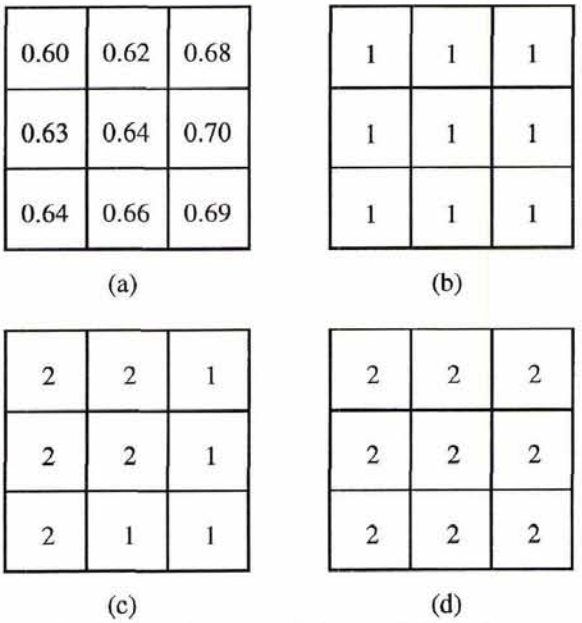

Figure 6. Class assignment within one field in the case of two classes: first likelihood probability (a), class assignment for $r = 0.55$ (b), $r = 0.65$ (c), $r = 0.75$ (d).

TABLE 3. MEAN AREA (m) AND STANDARD DEVIATION (σ) FOR EACH LAND-COVER CLASS AFTER 200 SIMULATIONS (HA)

m	forest	grassland	agriculture	built-up land	water
per field (1st)	1084.76	3780.45	8790.81	3101.99	141.95
per field (1st, 2nd)	1083.49	3781.88	8788.97	3103.70	141.95
per field (1st, 2nd, 3rd)	1083.81	3781.47	8790.11	3102.66	141.95
per field (1st, 2nd, 3rd, 4th)	1083.92	3781.38	8790.82	3101.92	141.97
per pixel	1083.82	3781.61	8790.42	3102.21	141.95
σ	forest	grassland	agriculture	built-up land	water
per field (1st)	53.93	107.90	176.97	189.45	2.18
per field (2st, 2nd)	11.23	30.16	48.93	47.20	1.21
per field (1st, 2nd, 3rd)	10.17	29.31	31.63	25.94	0.87
per field (1st, 2nd, 3rd, 4th)	8.58	28.33	29.55	24.26	0.87
per pixel	3.28	5.35	6.25	6.28	0.39

maining 30 percent to the second most likely class ($r > 0.70$).

Results and Discussion

Five simulation strategies have been applied, all based on the class membership probabilities generated by the fuzzy robust classifier yet using a different number of likelihood classes for the segmentation of the image. Table 3 reports area and standard deviation for the five major types of land cover after 200 simulations. As expected, the method of simulation has no impact on the assessment of area itself. Area estimates do not significantly differ from the estimates that were calculated directly from Equation 13 (Table 2). This shows that class membership probabilities for individual pixels are respected across realizations. Yet the assessment of uncertainty in the determination of area, as reported by the standard deviation, produces rather different results, depending on the simulation strategy that is applied. If pixels are independently assigned, as has so far been done in most studies on the modeling of error in classified imagery, standard deviation is small. At first sight this might give the impression that area estimates are quite reliable. If modeling is based on fields, however, the standard deviation is substantially higher. The way in which fields are defined plays an important part. If segmentation is solely based on the identity of the most likely class, standard deviation is very high. As more classes are involved in the definition of a field, the number of fields identified in the image will increase (Table 4) and the standard deviation will decrease accordingly.

The question that is raised at this point is, of course, which of the applied simulation strategies will give the best indication of area uncertainty or, in other words, which strategy best models the spatial structure of spectral response. In this context it is interesting to have a closer look at the membership probabilities for each of the classes. As was mentioned earlier class membership values indicate to what extent the first, second, third, and so on most likely class contribute to the spectral characteristics of a pixel.

Table 5 shows that for practically all pixels in the image (99.4 percent) the cummulated probability of the three most likely classes exceeds 0.95. One may therefore assume that the remaining two classes do not add significantly to the identification of the field structure. This is confirmed by the spatial characteristics of the likelihood images (Figure 1). While the third likelihood image still has a spatial structure that can easily be associated with the detailed pattern of land cover also found in the first and second likelihood image, the fourth likelihood image shows large patches of uniform land cover with grassland dominating in the northern part of the image and forest in the southern part. In the fifth likelihood image (which is not shown here), the majority of pixels is attributed to water. Water is the class with the most distinctive signature and is therefore not surprisingly the least likely class for almost all pixels that belong to other cover types. Using the fourth likelihood image in the segmentation does not lead to a major increase in the number of fields (Table 4) and therefore has a relatively small impact on the assessment of uncertainty compared with the results obtained with the three most likely classes. From this it can be concluded that the standard deviations which are obtained from the simulation that is based on the use of the three most likely classes offer a good indication of the uncertainty in area estimation.

As was mentioned before, the strategy for uncertainty modeling that is presented can also be applied in connection with inverse area calibration. In that case the segmented image can be obtained in exactly the same way as above, using the class membership probabilities produced by the maximum-likelihood classifier. For the simulation of land cover for each field, however, probabilities will be derived from the confusion matrix (see Equation 12). More in particular, if a field is classified into class j, random simulation for the pixels belonging to that field will be based on the probabilities found in the j-th column of the conditional probability matrix ($\mathbf{C}'\mathbf{R}^{-1}$). Because the segmentation strategy implies that all pixels that belong to the same field are also part of the same class in the original classification, conditional probabilities for these pixels will be equal. Hence, the entire field will be allocated to one class in the simulated image. This is in contrast to simulation based on maximum-likelihood probabilities, where pixels that belong to the same field may be allocated to different classes because their probability vectors are different (Figure 6).

If simulation is based on conditional probabilities derived from the confusion matrix, one may also use alternative strategies for the segmentation of the image. The segmentation method that has been presented in this paper works well with a small number of classes. However, as the number of classes increases, the image structure that is obtained will become more fragmented and larger fields may include a lot of small, isolated clusters of pixels that are not part of the actual structure of the land-cover scene. A variety of segmentation methods have been described in remote

TABLE 4. NUMBER OF FIELDS FOR DIFFERENT SEGMENTATION STRATEGIES

strategy	number of fields
1st	14932
1st, 2nd	50371
1st, 2nd, 3rd	71037
1st, 2nd, 3rd, 4th	77649
per pixel	422500

sensing literature to extract homogeneous regions from spatially heterogeneous classifications, using spectral and/or texture data (Haralick and Shapiro, 1985; Ryherd and Woodcock, 1996). All of these methods can be applied in combination with the approach for uncertainty modeling that is proposed in this study. Alternatively, the field structure can also be obtained by digitizing field boundaries from existing maps, or by extracting them from existing spatial databases, assuming that up-to-date information of this kind is readily available. However, it is important to note that the method for uncertainty modeling that is proposed assumes that only one image class occurs within the boundaries of each field. Indeed, this is the main justification for the stochastic modeling of uncertainty at the field level. If segmentation and classification are carried out independently, this *one field-one class* relationship cannot be guaranteed. Hence, per-field simulation of uncertainty using other segmentation strategies than the one that has been proposed will only work well if a post-classification phase is involved in which each segment (field) is allocated to exactly one image class. This combined segmentation-classification approach is often applied in remote sensing studies (Janssen *et al.*, 1990; Gong and Howarth, 1992; Fung and Chan, 1994; Johnsson, 1994).

An important issue in the kind of simulation modeling that is applied in this study is the determination of the minimum number of realizations that is necessary to obtain reasonable estimates of area and its associated uncertainty. Both are estimated by the sample mean and sample variance which are obtained after repeating the simulation process a fixed number of times. Expressions have been derived to calculate the variance of these estimators (Heuvelink, 1993). Both are inversely related to the number of realizations. The problem with these expressions, however, is that they are also dependent on the output variance of the simulation process which, of course, is not exactly known. That is why in this study the required number of realizations was derived experimentally. To get an idea of the variation in the sample variance, the Monte Carlo method was repeated ten times and this for 20, 50, 100, 150, and 200 realizations, respectively. For 200 realizations, the coefficient of variation of the sample variance proved to be below 0.05 for all types of land cover, at least for the experiments where image segmentation was based on more than two classes. This result was considered satisfactory to allow some trust to be put in the outcome of the uncertainty assessment.

Conclusion

With the increasing use of GIS, there is a greater concern for spatial data quality and a growing awareness that GIS technology can only reach its potential if the appropriate tools are provided to associate confidence limits with the output of a GIS analysis. The most important obstacle when handling uncertainty in geographical information systems is the lack of knowledge about the error present in the source data. When working with existing cartographic material, the information on data quality is usually sparse. Map making involves different data collection, generalization, and representation procedures, sometimes of a high level of abstraction, all leading to a degradation of data quality that is not easily described in a formal way. It is therefore clear that the key to a better understanding and modeling of source errors in GIS lies in the reduction of the level of abstraction in GIS databases (Goodchild and Wang, 1988). In this respect, the integrated use of digital satellite data in a GIS environment offers interesting challenges. Indeed, when using fuzzy classification approaches, class membership values indicating to what extent a pixel is likely to belong to each of the classes in the image can be derived. Being available for each pixel, these membership values provide valuable information with respect to the spatial structure of uncertainty in the classified image.

In this paper it has been demonstrated how class membership values can be used in the estimation of area for different land-cover classes as well as in the assessment of the uncertainty of these area estimates. Applying four variants of the maximum-likelihood classifier, it has been shown that the method which is used for the training of the classifier may have a considerable impact on the estimation of area, especially for classes with less distinctive signatures. A new method for the stochastic modeling of classification uncertainty has been proposed which makes optimal use of the class membership values derived from the classification. The method is based on the segmentation of the image in so-called "fields," i.e., groups of adjacent pixels with similar class membership values. Instead of looking at the uncertainty for each individual pixel, the fields in the segmented image are considered as the elementary spatial units in the error simulation process. Using different strategies for image segmentation, it has been made clear that the spatial characteristics of classification uncertainty have a strong impact on the assessment of the uncertainty of area estimates. This stresses the importance, as also mentioned by other authors, of properly dealing with the spatial structure of uncertainty in stochastic error modeling. Although the assumption that classification uncertainty is field-based rather than pixel-based is justified for agricultural areas, it is important to mention that it is probably not a useful strategy to apply in areas with semi-natural vegetation where classes tend to inter-grade gradually. Here, the use of a continuous model of spatial variation or a combination of both discrete and continuous modeling may be more appropriate.

TABLE 5. PROPORTION OF THE TOTAL NUMBER OF PIXELS IN EACH PROBABILITY CLASS FOR DIFFERENT SEGMENTATION STRATEGIES (PERCENTAGES REFER TO THE CUMMULATED PROBABILITY FOR ALL THE CLASSES INVOLVED IN THE SEGMENTATION OF THE IMAGE)

	0.20–0.49	0.50–0.74	0.75–0.94	0.95–0.99	1.0
1st	2.8	17.9	23.8	22.7	32.8
1st + 2nd	0.0	0.7	11.8	26.4	61.1
1st + 2nd + 3rd	0.0	0.0	0.6	12.9	86.5
1st + 2nd + 3rd + 4th	0.0	0.0	0.0	9.4	90.6

Acknowledgments

This research is part of the Belgian Scientific Research Programme on Remote Sensing by Satellite - phase three (Federal Office for Scientific, Technical and Cultural Affairs), contract Telsat/III/03/004. The scientific responsability is assumed by its author. I would like to thank Dr. Raymond Czaplewski and two anonymous reviewers for their valuable comments. Thanks also go to Hans Dufourmont for the use of the Landsat data and the training sets, Johan Vandeneede for providing the source code for the maximum-likelihood classification, and Frank Forier who assisted in preparing the figures.

References

Bauer, M.E., M.M. Hixson, B.J. Davis, and J.B. Etheridge, 1978. Area estimation of crops by digital analysis of Landsat data, *Photogrammetric Engineering & Remote Sensing*, 44:1033–1043.

Bezdek, J.C., R. Ehrlich, and W. Full, 1984. FCM: The fuzzy c-means clustering algorithm, *Computers and Geoscience*, 10:191–203.

Brown, P.J., 1982. Multivariate calibration, *Journal of the Royal Statistical Society*, 44:287–321.

Brunsdon, C., S. Carver, M. Charlton, and S. Openshaw, 1990. A review of methods for handling error propagation in GIS, *Proceedings of*

the First European Conference on Geographical Information Systems, Amsterdam, The Netherlands, pp. 106–116.

Burrough, P.A., and A.U. Frank (editors), 1996. *Geographic Objects with Indeterminate Boundaries*, Taylor & Francis, London, UK, 345 p.

Campbell, N.A., 1980. Robust procedures in multivariate analysis I: Robust covariance estimation, *Applied Statistics*, 29:231–237.

Cannon, R.L., J.V. Dave, and J.C. Bezdek, 1986. Efficient implementation of the Fuzzy c-Means Clustering Algorithm, *IEEE Transactions on Pattern Recognition and Machine Intelligence*, 8:248–255.

Canters, F., 1994. Simulating error in triangulated irregular network models, *Proceedings of the Fifth European Conference and Exhibition on Geographical Information Systems*, Paris, France, pp. 169–178.

Card, D.H., 1982. Using known map categorical marginal frequencies to improve estimates of thematic map accuracy, *Photogrammetric Engineering & Remote Sensing*, 48:431–439.

Congalton, R.G., 1988. A comparison of sampling schemes used in generating error matrices for assessing the accuracy of maps generated from remotely sensed data, *Photogrammetric Engineering & Remote Sensing*, 54:593–600.

Czaplewski, R.L., and G.P. Catts, 1992. Calibration of remotely sensed proportion or area estimates for misclassification error, *Remote Sensing of Environment*, 39:29–43.

Fisher, P.F., 1991. Modelling soil map-unit inclusions by Monte Carlo simulation, *International Journal of Geographical Information Systems*, 5:193–208.

———, 1992. First experiments in viewshed uncertainty: Simulating fuzzy viewsheds, *Photogrammetric Engineering & Remote Sensing*, 58:345–352.

———, 1994. Visualization of the reliability in classified remotely sensed images, *Photogrammetric Engineering & Remote Sensing*, 60:905–910.

Fisher, P.F., and S. Pathirana, 1990. The evaluation of fuzzy membership of land-cover classes in the suburban zone, *Remote Sensing of Environment*, 34:121–132.

———, 1993. The ordering of multitemporal fuzzy land-cover information derived from Landsat MSS data, *Geocarto International*, 8:5–14.

Foody, G.M., 1992. On the compensation for chance agreement in image classification accuracy assessment, *Photogrammetric Engineering & Remote Sensing*, 58:1459–1460.

———, 1994. Ordinal-level classification of sub-pixel tropical forest cover, *Photogrammetric Engineering & Remote Sensing*, 60:61–65.

Foody, G.M., N.A. Campbell, N.M. Trodd, and T.F. Wood, 1992. Derivation and applications of probabilistic measures of class membership from the maximum-likelihood classification, *Photogrammetric Engineering & Remote Sensing*, 58:1335–1341.

Fung, T., and K. Chan, 1994. Spatial composition of spectral classes: A structural approach for image analysis of heterogeneous land-use and land-cover types, *Photogrammetric Engineering & Remote Sensing*, 60:173–180.

Gong, P., and P.J. Howarth, 1992. Land-use classification of SPOT HRV data using a cover-frequency method, *International Journal of Remote Sensing*, 13:1459–1471.

Goodchild, M.F., and M.-H. Wang, 1988. Modeling error in raster-based spatial data, *Proceedings of the Third International Symposium on Spatial Data Handling*, Sydney, Australia, pp. 97–106.

———, 1989. Modeling errors for remotely sensed data input to GIS, *Proceedings of the Ninth International Symposium on Computer-Assisted Cartography*, Baltimore, Maryland, pp. 530–537.

Gopal, S., and C. Woodcock, 1994. Theory and methods for accuracy assessment of thematic maps using fuzzy sets, *Photogrammetric Engineering & Remote Sensing*, 60:181–188.

Green, E.J., W.E. Strawderman, and T.M. Airola, 1993. Assessing classification probabilities for thematic maps, *Photogrammetric Engineering & Remote Sensing*, 59:635–639.

Haralick, R.M., and L.G. Shapiro, 1985. Survey: Image segmentation techniques, *Computer Vision, Graphics, and Image Processing*, 29: 100–132.

Heuvelink, G.B.M., 1993. *Error Propagation in Quantitative Spatial Modeling, Applications in Geographical Information Systems*, KNAG/Netherlands Geographical Studies, Utrecht, The Netherlands, 151 p.

Heuvelink, G.B.M., P.A. Burrough, and H. Leenaers, 1990. Error propagation in spatial modeling with GIS, *Proceedings of the First European Conference on Geographical Information Systems*, Amsterdam, The Netherlands, pp. 453–462.

Janssen, L.L.F., M.N. Jaarsma, and E.T.M. van der Linden, 1990. Integrating topographic data with remote sensing for land-cover classification, *Photogrammetric Engineering & Remote Sensing*, 56:1503–1506.

Janssen, L.L.F., and F.J.M. van der Wel, 1994. Accuracy assessment of satellite derived land-cover data: A review, *Photogrammetric Engineering & Remote Sensing*, 60:419–426.

Johnsson, K., 1994. Segment-based land-use classification from SPOT satellite data, *Photogrammetric Engineering & Remote Sensing*, 60:47–53.

Lee, J., P.K. Snyder, and P.F. Fisher, 1992. Modeling the effect of data errors on feature extraction from digital elevation models, *Photogrammetric Engineering and Remote Sensing*, 58:1461–1467.

Maselli, F., C. Conese, and L. Petkov, 1994. Use of probability entropy for the estimation and graphical representation of the accuracy of maximum likelihood classifications, *ISPRS Journal of Photogrammetry and Remote Sensing*, 49:13–20.

Mowrer, H.T., 1994. Monte Carlo techniques for propagating uncertainty through simulation models and raster-based GIS, *Proceedings of the International Symposium on Spatial Accuracy of Natural Resource Data Bases*, Williamsburg, Virginia, pp. 179–188.

Pech, R.P., A.W. Davis, R.R. Lamacraft, and R.D. Graetz, 1986. Calibration of LANDSAT data for sparsely vegetated semi-arid rangelands, *International Journal of Remote Sensing*, 7:1729–1750.

Prisley, S.P., and J.L. Smith, 1987. Using classification error matrices to improve the accuracy of weighted land-cover models, *Photogrammetric Engineering & Remote Sensing*, 53:1259–1263.

Richards, J.A., 1986. *Remote Sensing Digital Image Analysis, An Introduction*, Springer-Verlag, Berlin, Germany, 281 p.

Rosenfield, G.H., K. Fitzpatrick-Lins, and H.S. Ling, 1982. Sampling for thematic map accuracy testing, *Photogrammetric Engineering & Remote Sensing*, 48:131–137.

Ryherd, S., and C. Woodcock, 1996. Combining spectral and texture data in the segmentation of remotely sensed images, *Photogrammetric Engineering & Remote Sensing*, 62:181–194.

Stehman, S.V., 1992. Comparison of systematic and random sampling for estimating the accuracy of maps generated from remotely sensed data, *Photogrammetric Engineering & Remote Sensing*, 58:1343–1350.

———, 1995. Thematic map accuracy assessment from the perspective of finite population sampling, *International Journal of Remote Sensing*, 16:589–593.

Strahler, A.H., 1980. The use of prior probabilities in maximum likelihood classification of remotely sensed data, *Remote Sensing of Environment*, 10:135–163.

Strahler, A.H., C.E. Woodcock, and J.A. Smith, 1986. On the nature of models in remote sensing, *Remote Sensing of Environment*, 20:121–139.

Vandeneede, J., F. Fierens, P. Dewaele, P. Wambacq, and A. Oosterlinck, 1995. Development of image processing software in the Telsat/II/12 program, *Space Scientific Research in Belgium, Volume III: Earth Observation, Part 1*, Federal Office for Scientific, Technical and Cultural Affairs, Brussels, Belgium, pp. 71–88.

van Genderen, J.L., B.F. Lock, and P.A. Vass, 1978. Remote sensing: statistical testing of thematic map accuracy, *Remote Sensing of Environment*, 7:3–14.

Walsh, T.A., and T.E. Burk, 1993. Calibration of satellite classifications of land area, *Remote Sensing of Environment*, 46:281–290.

Wang, F., 1990a. Fuzzy supervised classification of remote sensing images, *IEEE Transactions on Geoscience and Remote Sensing*, 28:194–201.

———, 1990b. Improving remote sensing image analysis through fuzzy information representation, *Photogrammetric Engineering & Remote Sensing*, 56:1163–1169.

(Received 11 December 1995; revised and accepted 18 April 1996; revised 19 June 1996)